



Effect of powder particle size distribution on the surface finish of components manufactured by laser powder bed fusion

Sara Sendino¹ · Silvia Martinez¹ · Fernando Lartategui² · Marc Gardon³ · Aitzol Lamikiz¹ · Javier Jesus Gonzalez⁴

Received: 1 July 2022 / Accepted: 31 October 2022 / Published online: 25 November 2022
© The Author(s) 2022

Abstract

One of the key aspects of the laser powder bed fusion (L-PBF) process is the quality of the raw powder since it affects the final properties of the manufactured parts. In this study, 13 batches of Inconel® 718 powder were analysed, all of them being specially designed for L-PBF technology and meeting similar requirements but coming from different suppliers. Therefore, these batches have certain differences in their characteristics, including the particle size distribution (PSD). This study presents the relationship between the PSD of each batch and the surface roughness obtained in the manufactured parts. For the roughness study, Sa and Sz parameters are presented; in addition, the size and frequency of the particles adhered to the surface were quantified, and an autocorrelation analysis was carried out. Furthermore, after this analysis, the parts were sandblasted in order to repeat the same analysis after removing the adhered particles from the surface. This work points to the fact that the particles adhered to the surface are the smallest particles in the powder batch, and their size affects the roughness of the final part. This means that the surface roughness is strongly related to the fraction of smaller particles within the PSD of the batch, while there is no relationship between the surface roughness and the larger particles.

Keywords Laser powder bed fusion · Roughness · Adhered particles · Surface · Powder particle size distribution

1 Introduction

Laser powder bed fusion (L-PBF) technology is one of the additive manufacturing (AM) technologies that have been most developed in recent years for the manufacture of functional metal parts [1]. This is due to its better surface quality and higher dimensional accuracy compared to other AM technologies [2], as well as the ability to manufacture very complex structures [3]. These advantages make this

technology very attractive for certain sectors, such as the aerospace and medical industries where weight reduction is crucial [3].

For the manufacture of these components, metal powder is supplied directly into the manufacturing chamber layer-by-layer. Layer thickness is selected depending on the required surface finishing, and it is usually between 20 and 60 µm [4]. Once each layer is spread, a laser beam melts the area specified in the trajectories file, melting the powder and forming a solidified area of the part. Finally, the platform decreases the layer thickness, and a new layer of powder is spread. The process is repeated until the build is complete.

Despite advancements made in recent years, this technology still has some disadvantages; one of them is the poor surface finish of the parts. This high roughness generates a lower fatigue strength [5, 6] or even the proliferation of different microorganisms [7]. Therefore, the factors that generate high roughness are the focus of many studies.

Some works, such as the studies carried out by Rott et al. [8] or Senin et al. [9], divide the surface roughness of L-PBF parts into two types: patterns due to the solidification of the melt pool and particles adhered to the part surface. The origin of these two types of roughness is due to different factors.

✉ Sara Sendino
sara.sendino@ehu.eus

¹ Department of Mechanical Engineering, Aeronautics Advanced Manufacturing Center (CFAA), University of the Basque Country (UPV/EHU), P. Tecnológico de Bizkaia, 202, 48170 Zamudio, Spain

² ITP Aero, P. Tecnológico de Bizkaia, 300, 48170 Zamudio, Spain

³ Renishaw Ibérica, Carrer de La Recerca, 7, 08850 Gavà, Barcelona, Spain

⁴ Department of Mining Engineering and Metallurgy and Materials Science, University of the Basque Country (UPV/EHU), Plaza Torres Quevedo 1, 48013 Bilbao, Spain

The roughness pattern due to the solidification of the melt pool is usually associated with the layer height [10] or the angle of incidence of the laser [11]. On the one hand, the layers are perceived on the surface of the final part; therefore, the thicker the layers, the greater the roughness [10]. On the other hand, the angle of incidence of the laser depends on the positioning of the part on the platform [12, 13]. The scanner mirrors are usually positioned just above the central part of the platform. Due to this positioning, the laser beam is perpendicular to the platform only in the central part, as the studies carried out by Rott et al. [8] demonstrated. While on the parts located far from the centre of the platform, the laser beam is not completely perpendicular [11, 14] to the platform so, it generates distortion in the melt pool that affects the roughness of the final part [15].

Finally, in the case of particles adhered to the surface, it should be noted that there are different types of particles adhered according to Nasab et al. [16]. There are particles that belong to the powder batch that melted and adhered to the surface; therefore, these particles have a size according to the initial powder particle size distribution (PSD). On the contrary, there are spatters which usually have a larger size (around 200 μm) and a different microstructure from the rest of the part.

Several factors affect the number and size of these adhered particles such as the proximity between parts [7], the inert gas flow inside the manufacturing chamber [17], the positioning of the part with respect to the recoater [18], and the properties of the raw powder [19]. Previous studies have shown that the presence of adhering particles on the surface of parts manufactured by L-PBF depends mainly on the temperature of the powder layer. Thus, as the temperature of the powder layer increases, the presence of adhering particles increases [20].

The characteristics of the raw powder influence strongly the quality of the final part [19]. PSD affects the surface finish because powders with coarser particles result in a rougher surface [21]. It should be noted that PSD is not homogenous across the whole layer. Since the recoater tends to deposit the smallest particles at the beginning of the platform, the largest ones are deposited at the end [13, 18]. The morphology of the powder particles also affects the surface finish. The less spherical the particles are, the higher the roughness of the surface will present [3]. The spatters created in the powder bed also cause an increase in roughness [7]. The concentration of spatter is not homogeneous in the powder bed since the inert gas flow inside the manufacturing chamber transports these oxidized particles out of the processed area.

Finally, other factors that affect roughness are the geometry of the part itself, whether it is a surface with previously melted material underneath (upskin, not downskin) [22], and the process parameters used to manufacture the part [4].

When the laser energy density is high, roughness tends to decrease due to the increased wettability of the layers [23]. However, high energy density also generates more spattering causing the roughness to increase [24]. Consequently, it is necessary to seek a balance between laser power and scanning speed in order to ensure acceptable roughness properties among other final part properties [25].

Throughout this study, a relationship between the PSD of each batch and the surface roughness obtained in the manufactured parts is presented. For this purpose, 13 different powder batches were analysed, and their PSD was then related to the characteristics of the surface finish and roughness obtained in each sample.

2 Materials and methods

For this study, 13 virgin batches of Inconel® 718 powder from different suppliers were analysed and labelled from IN01 to IN13. According to the suppliers' specifications, all batches met the necessary requirements in terms of characteristics such as PSD, morphology, and composition and were suitable for use in the L-PBF process. During this procedure, in order to avoid cross-contamination caused by other batches or moisture, the batches were stored in specific, hermetically sealed containers until they were opened for analysis and manufacture.

The study was divided into four main sections. First, the PSD of the powder batches was determined, and then the samples were manufactured for subsequent roughness analysis. Once the roughness was analysed and related to the PSD of the powder batch, the parts were sandblasted to analyse the surface again.

2.1 Particle size distribution (PSD)

A correct determination of PSD is crucial for the studies to be carried out properly, so despite having the data provided by the suppliers, the PSD was re-analysed according to ISO 13320 by laser diffraction.

Thanks to this study, D_{sub} values were obtained, which indicate the point in the size distribution to the specified volume percentage. For example, if D_{50} is 42 μm , this means that 50% of the total volume of particles is equal or smaller than 42 μm .

2.2 Manufacture of samples

The samples for this study were manufactured on a Renishaw AM400 manufacturing system, and QuantAM V4 software was used to program the parameters.

The objective of this work is to determine the effects caused by the characteristics of the different powder batches

on roughness. For that reason, the same part geometry and parameters were used with all batches.

The manufacture of each layer can be divided into two steps. First, the inner volume of the part is processed using a filling stripes strategy with a given hatching distance between the laser paths. Subsequently, with the objective of improving the surface finish, the contours of the layer are processed. The volume and contour parameters are presented in Table 1, and a schematic of the strategy is shown in Fig. 1.

Roughness is due to many factors, not only of the characteristics of the powder batch used or parameters. In order to limit the roughness caused by those factors as much as possible, the samples designed were rectangular geometries to avoid using both upskin and downskin surfaces (Fig. 1). Additionally, they were located in the central part of the platform, thus obtaining a laser beam completely perpendicular to the platform.

The samples were manufactured from batches IN01 to IN13. It should be noted that after manufacturing with each batch, the machine was completely emptied and cleaned to avoid cross-contamination.

2.3 Surface finish and sample roughness

The roughness analysis was divided into four sections. First, the surface roughness was analysed by means of the arithmetical mean height (Sa) and maximum height (Sz) parameters. Then, taking into account the relationship obtained between the roughness and the PSD of the powder batches, the particles adhered to the surface were analysed.

In addition, to obtain a more detailed analysis of the surface, an autocorrelation analysis was carried out and spatial parameters were obtained. Finally, a metallographic analysis of the particles adhered to the surface was carried out.

2.3.1 Surface roughness analysis

Roughness was measured on the four vertical faces of the sample, to elude the effects of the argon flow and recoater direction.

To analyse the surface finish of the part, Sa and Sz parameters were studied, in accordance with ISO 25178–2. A non-contact system was used to carry out the measurements, specifically, an infinite focus microscope (Alicona Infinite Focus Microscope Model Control ServerFP G1 Vf2) and the roughness analysis was performed using the tools provided by the laboratory measurement module (MSURF software). Thanks to this system, the topographies of the surfaces were also obtained.

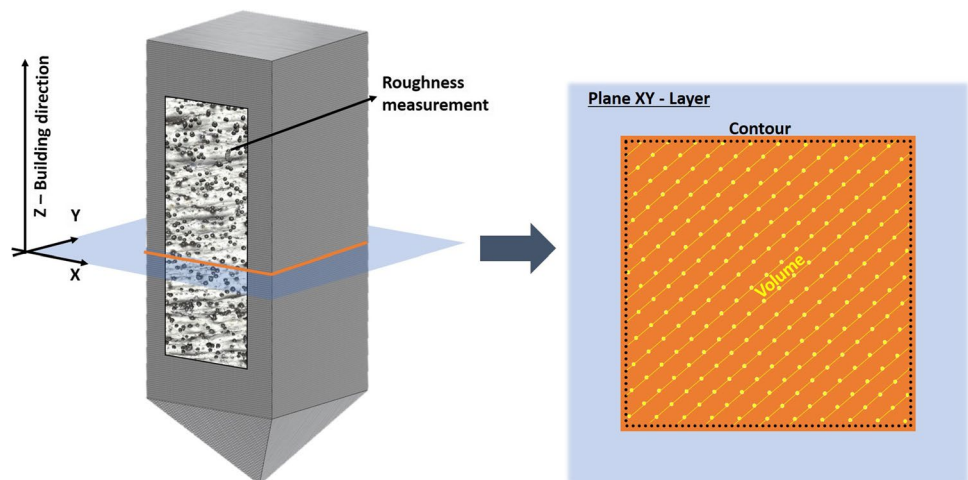
2.3.2 Analysis of particles adhered to the surface

Based on the obtained topographic images, particles adhered to the surface were analysed to check their size. To carry out this study, different L and F filters were applied to the topography to obtain a surface where it was possible to isolate the adhered particles. This filtering was performed directly using MSURF software, and the result is shown in Fig. 2(a).

Table 1 Volume and border parameters used

	Layer thickness [μm]	Power [W]	Exposure time [μs]	Point distance [μm]	Hatch distance [μm]	Strategy angle [°]
Volume	60	200	70	80	80	67
Contour		125	75	20	-	-

Fig. 1 Schematic of the contour and volume strategies followed on the part



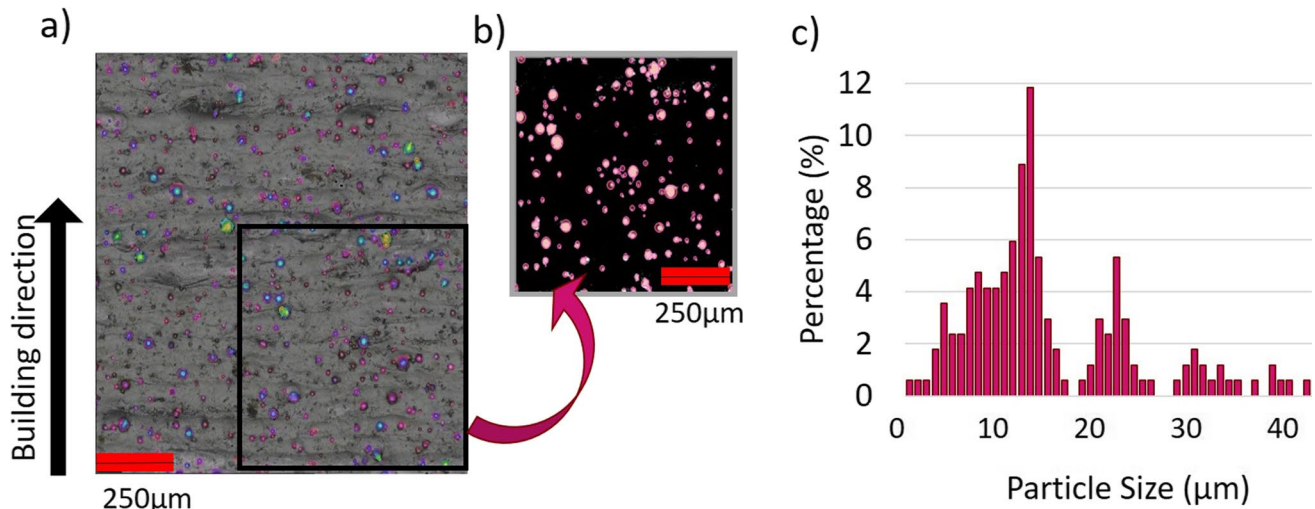


Fig. 2 Analysis of particles adhered to the surface: **a** the filtered surface, ready for MATLAB® analysis, **b** isolated particles, and **c** histogram to analyse the adhered particles size distribution

Once the surface was filtered, the particles were analysed by a digital image processing software developed in MATLAB®. Using this software, it is possible to detect the contours of the particles on the topography, thanks to their small size and high circularity (Fig. 2(b)).

Finally, the diameter of each adhered particle was determined, and a histogram was obtained where the size distribution of the particles adhered to the surface could be analysed (Fig. 2(c)).

2.3.3 Analysis of surface autocorrelation and spatial parameters

Autocorrelation analysis, defined in the ISO 25178 standard, is used to study the relationship between the original surface and the same surface translated in X- and Y-axes. Thanks to this analysis, it can be determined how uniform the surface is. This autocorrelation function is defined in the following equation, where A is the analysed surface and t_x and t_y are the surface displacements in each case:

$$f_{ACF}(t_x, t_y) = \frac{\iint_A z(x, y)z(x - t_x, y - t_y)dx dy}{\iint_A z(x, y)z(x, y)dx dy} \quad (1)$$

Finally, in order to analyse the presence of layers on the surface, the parameter called surface texture direction (Std), which indicates the predominant direction of the surface texture, was used. In the parts manufactured using L-PBF technology, this direction is the direction of layer growth.

This parameter is a measure of the angular direction of the dominant directions in the surface. Leach [26] explained that Std is calculated from the Fourier spectrum after applying the

radial integration method. Thanks to this spectrum, it can be determined which directions are predominant on the surface.

Using this spectrum and taking into account all the predominant directions of the surface, it can be calculated how important the analysed direction is. For this purpose, the parameter Stdi was used. The smaller the value of this parameter, the stronger the directionality of the structure.

Thus, the Std value indicates the angular direction of the predominant surface texture direction, while the Stdi parameter indicates how important this direction is compared to the rest.

To conclude the roughness analysis, the bearing area curve (also known as the Abbott Firestone Curve) was analysed. This surface analysis was also carried out, as defined in the ISO 25178 standard, using MSURF software.

Mathematically, the bearing area is established by evaluating the material ratio (mr) at various levels from the highest peak to the lowest valley. This results in the cumulative probability density function of the different surface heights [27].

This curve is divided into three zones: the peak zone ($mr1 = 10\%$), the core zone, and the valley zone ($mr2 = 80\%$). This study was focused only on the peak zone, and the parameter V_{mp} (peak material volume) was analysed. This parameter represents the volume of material from the core of the material to the highest peak of the surface. This parameter increases if there is more volume belonging to the peaks; this may be due to more particles on the surface or coarser particles.

2.3.4 Metallographic analysis of particles adhered to the surface

A metallographic analysis of the adhered particles was carried out. For the correct analysis of these samples, they were first cut to analyse the XZ plane (the Z-axis being the build direction,

perpendicular to the layers). Then, the samples were encapsulated using phenolic resin. After that, the planar grinding step was performed using silicon carbide and corundum sandpaper (using FEPA400, FEPA600, FEPA800, and FEPA 1200 grain sizes). Once the surface was ready, it was polished using 1 μm and 3 μm polycrystalline diamond powder. Once the mirror-finish surface was achieved, surface images were taken using the infinity focus microscope with 50 \times magnification.

Finally, the samples were etched using Marble’s Reagent (whose chemical composition is 10 g CuSO_4 , 50 ml HCl , 50 ml H_2O , as specified in ASM 1998 standard) to analyse the microstructure of the parts and check the fusion between the adhered particle and the part surface.

2.4 Analysis of the final parts after sandblasting

The Euroblast Euro4SF blasting system using white corundum WSK 80 was used to sandblast the samples. In order to blast all parts uniformly, each surface of the part was blasted for 3 s.

Surface roughness was analysed again, following the same procedure for each part by means of the S_a and S_z parameters. The autocorrelation was also examined to check how the surface changed after blasting.

3 Results and discussion

The results are divided into three sections: PSD analysis, roughness analysis, and roughness analysis after blasting the parts.

3.1 Particle size distribution (PSD)

Figure 3(a) exhibits the PSD results obtained from the 13 powder batches, and several differences are observed between them. For example, within the small particle fraction of the distribution (D_1 – D_{10}), the particles are larger in

size in batches IN03 and IN08, while batches IN11 and IN13 contain the smallest particle sizes.

In Fig. 3(b) three of the powder batches with the greatest differences are shown (batches IN07, IN08, and IN13 were selected for this analysis) and depict how some batches present a more homogenous PSD. Specifically, IN08 is the batch that has the most homogeneous PSD of the 13 batches tested, since the smallest particles of the batch (D_1) and the coarsest (D_{100}) have a difference of approximately 50 μm , while in batch IN13, this difference is around 71 μm . Thus, the medium particles in the distribution are closer in size to the smallest particles.

3.2 Surface finish and sample roughness

First, the surface roughness was analysed, and the S_a and S_z parameters were presented. Then, the size of the particles adhered to the surface was determined. Subsequently, the autocorrelation analysis and spatial parameters are presented. Finally, the metallographic analysis is shown.

3.2.1 Surface roughness analysis

Figure 4 shows the mean values of the parameters S_a in Fig. 4(a) and S_z in Fig. 4(b) for each of the powder batches.

As can be observed in Fig. 4, S_a values are between 6 and 9 μm while S_z values vary between 40 and 60 μm . This variation is due to the powder batch characteristics since both the parameters used during the manufacturing process and the platform design were identical in all cases.

Roughness parameters are represented together with the PSD values (D_1 , D_{10} , and D_{50}). This first analysis shows a relationship between the roughness and the PSD of the powder.

This relationship between the obtained S_a value and the PSD was checked (Fig. 5), and it shows a linear relationship between the roughness acquired and particle diameter in the case of the smallest particles of each batch (particles with a diameter smaller than D_{50}). This relationship shows that

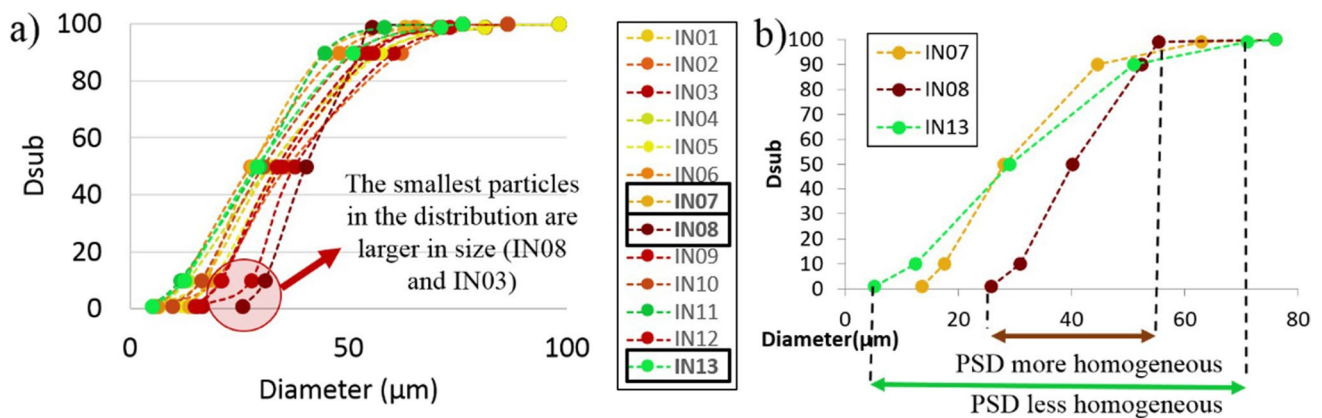


Fig. 3 a PSD analysis of the 13 batches of powder and b detail of some of the most representative batches

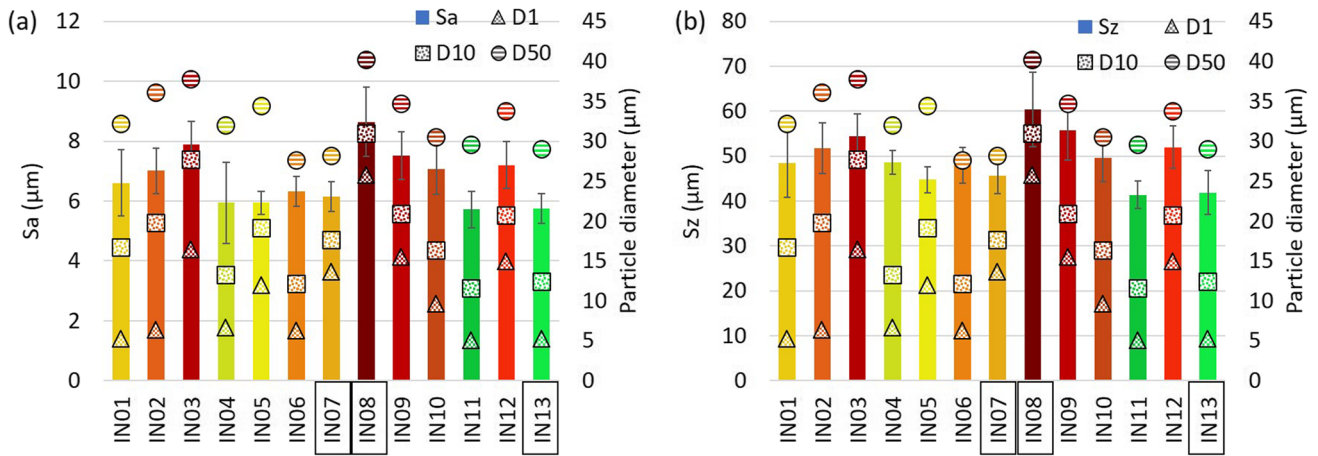
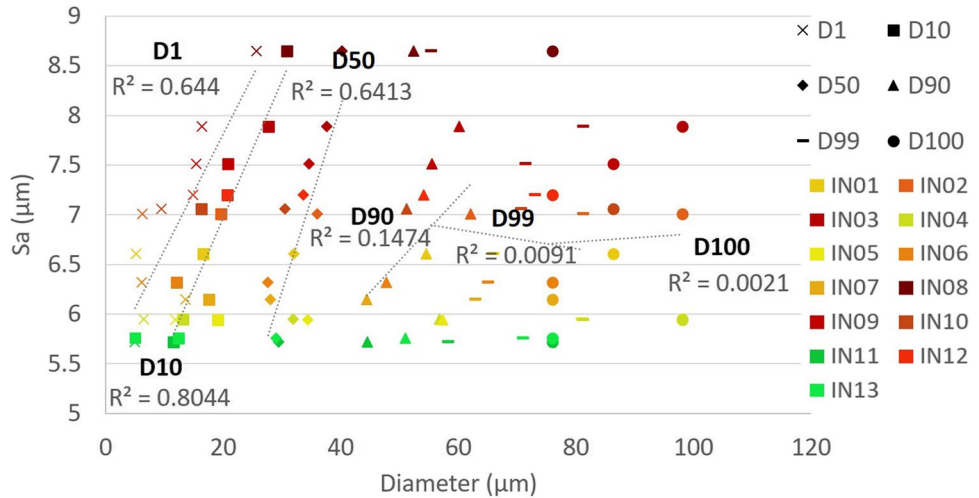


Fig. 4 Roughness analysis of parts and PSD values a Sa and b Sz

Fig. 5 Relationship between the obtained roughness values (*Sa*) and the particle diameters belonging to each *D_{sub}*



the smaller the size of the smallest particles in the batch, the lower the roughness.

Nevertheless, this relationship is only fulfilled in the case of groups *D₁*, *D₁₀*, and *D₅₀* and disappeared in the case of larger particles. Thus, there is no relationship between the coarsest particles of the distribution and the roughness of the final part.

3.2.2 Analysis of particles adhered to the surface

To check the relationship between the roughness of parts and the PSD, each of the surfaces was analysed using digital image processing software developed in MATLAB®.

Batches IN07, IN08, and IN13 were selected for the analysis of the particles adhered to the surface, as these batches showed the greatest differences in roughness values and in PSD. Specifically, IN08 is the batch that showed the highest roughness

when measuring the *Sa* and *Sz* values and the largest particles of the PSD, batch IN13 had the smallest particles and the lowest roughness, and finally, batch IN07 had a medium roughness and intermediate particle size. In some analyses, only the results obtained from these three batches are presented; however, the same study was carried out for all 13 batches.

In each case, a histogram depicts the percentage of adhered powder particles that exhibit a certain particle size. The batch that shows the largest adhered particles to the surface is batch IN08 (Fig. 6(b)). In this case, there are particles up to 47 µm, while in the case of batch IN13 (Fig. 6(c)), the adhered particles only reach diameters of approximately 33 µm. In the case of batch IN07 (Fig. 6(a)), the larger particles adhered to the surface are very similar to those exhibited by batch IN13. Although as it has a more homogeneous distribution, the percentage of larger particles adhered to the surface is higher, which increases its roughness. It should be

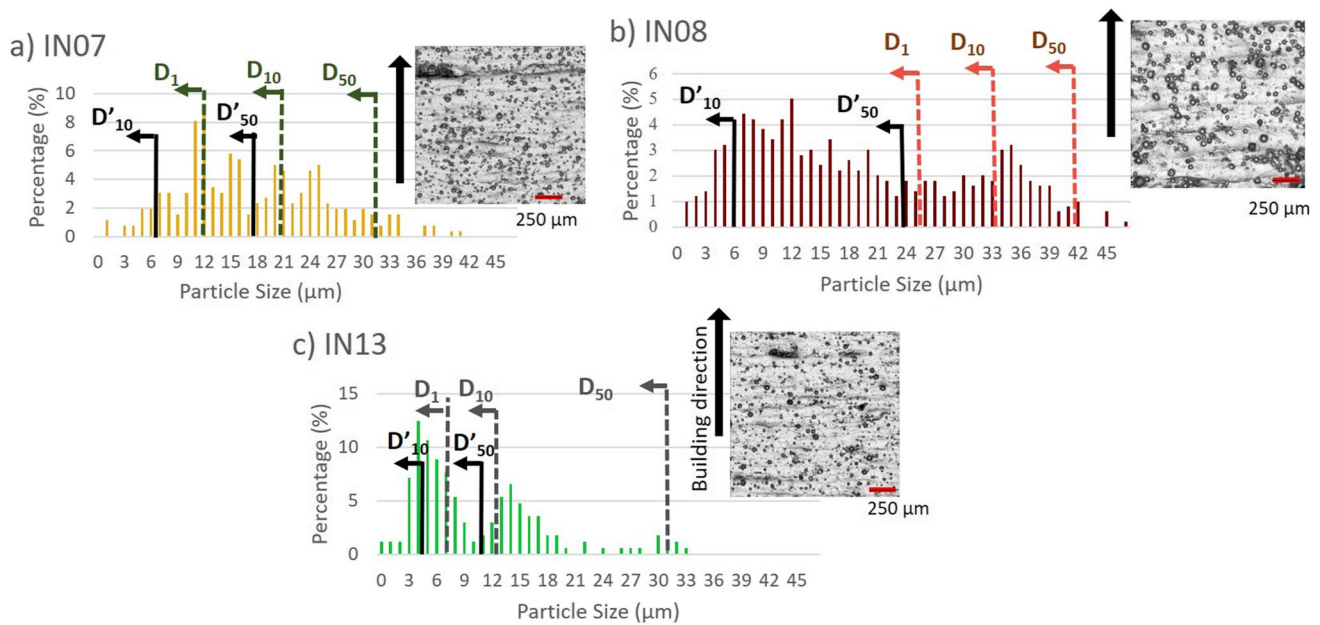


Fig. 6 Analysis of the particles adhered to the surface manufactured by the L-PBF technology: **a** results obtained with batch IN07—intermediate roughness, **b** batch IN08—high roughness, **c** batch IN13—low roughness

noted that in each case, the adhered particles always had a diameter similar or smaller than the respective D_{50} diameter of each batch.

In addition to the PSD of the powder (D_1 , D_{10} , or D_{50}), Fig. 6 shows the PSD of the particles adhered to the surface (D'_{10} , D'_{50}). As can be seen, in batch IN13, 50% of the adhered particles in the volume are smaller than 11 μm , while in the case of IN08 this value increases up to 25 μm .

Therefore, after this analysis, the results determine that the roughness due to adhered particles is caused only by the smallest particles of the PSD, as these are the ones that adhere to the surface.

3.2.3 Analysis of surface autocorrelation and spatial parameters

Figure 7 shows the autocorrelation diagrams obtained in the case of powder batch IN13 (Fig. 7(b)), whose surface showed the smallest particles adhered to the surface, and batch IN08 (Fig. 7(a)), whose surface showed larger particles. Both figures show that the total autocorrelation occurs only in the centre, before image translation (the red point in the middle of the autocorrelation diagram).

In the case of batch IN13, the small particles adhered to the surface allow the pattern composed of layers to remain visible, as can be seen in Fig. 7(b) below. After translating the image on the X-axis, the small particles do not correlate, but the layers do, and consequently the correlation increases. However, in the case of batch IN08, the larger

particles adhered to the surface hide the pattern composed of layers making this autocorrelation less evident.

Figure 7(c) shows the spatial parameters of the powder batches IN07, IN08, and IN13. The predominant direction on the surface is always 0° , as indicated by the Std parameter. This direction coincides with the direction of layer growth. Stdi shows how in the case of IN13 the direction of the layers is more evident since the particles do not hide the layers.

Finally, the Vmp parameter shows how, in the case of batch IN08, there is more material belonging to the peak volume. This is also appreciable in the bearing curve shown in Fig. 6(d).

3.2.4 Metallographic analysis of particles adhered to the surface

Figures 8(a) and (b) present the metallographic analysis carried out before etching the surface. In these images, different adhered spherical particles were evaluated, analysing their diameter and their attachment surface (Fig. 8(a)). It should be noted that the diameter analysed in the image is not the real diameter of the particle, as the diameter analysed in the image depends on the section made.

The images show how the resulting surface roughness is composed of both layers and spherical particles adhered to the surface (Fig. 8(b)). Then, the samples were etched (Fig. 8(c)), and it was found that the microstructure of the adhered particles is the same as the microstructure of the

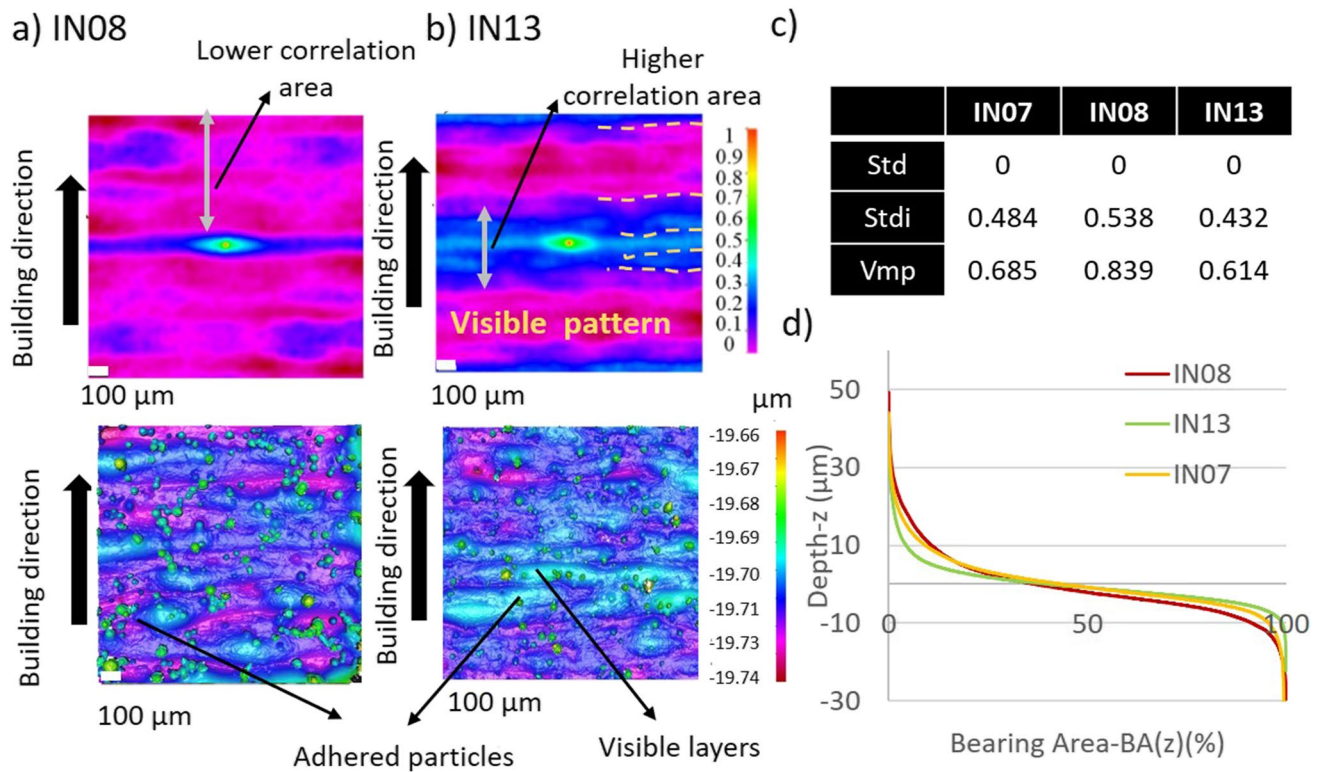


Fig. 7 Analysis of spatial parameters and autocorrelation of the surfaces: **a** above: autocorrelation diagram of batch IN08, where the direction of growth of the part is indicated. Below: surface image **b**

above: autocorrelation diagram of batch IN13. Below: surface image **c** analysed parameters and **d** bearing area curve

part, which shows that the particles come directly from the powder batch and that there are not oxidized particles or spatters.

Finally, particles belonging to the powder bed were analysed. The size of these particles is similar to those adhering to the surface. Furthermore, the microstructure of these particles was analysed, and it can be seen in Fig. 8 (c) and (d) how the microstructure of the particles is transformed due to the melting process on the part.

3.3 Analysis of the samples after sandblasting

In order to analyse the surface without the interference of the adhered particles, the samples' surfaces were sandblasted. By following this procedure, the adhered particles are removed while the melt layers remain on the surface.

3.3.1 Surface roughness analysis

Figure 9 shows the roughness values S_a and S_z obtained from the parts after being sandblasted. Roughness has greatly decreased and has become more homogeneous between different batches. Specifically, S_a values decreased by about 45% with values between 3 and 5 μm (Fig. 9(a))

while S_z values decreased by about 59% and the values obtained were between 18 and 25 μm (Fig. 9(b)).

In addition, topographic images of surfaces IN07, IN08, and IN13 are presented in Fig. 9(c). After being blasted, all parts show a very similar surface appearance, because the adhered particles were removed. Even so, after the blasting process, small differences in the surface images are still visible. These differences are the result of the marks left by the adhering particles when they are removed from the surface. Therefore, the presence of these surface marks is smaller on the batches with fewer or smaller particles (IN13), where the pattern composed of layers is more visible than in the case of batches with a higher number of adhering particles.

3.3.2 Analysis of surface autocorrelation and spatial parameters

Once the particles were removed from the surface, the autocorrelation diagrams show how the pattern composed of layers is more evident than in the case of the samples before blasting (Fig. 10(a) and (b)). Moreover, all the surfaces were homogenized considerably, as seen in the previous analysis of the S_a and S_z parameters.

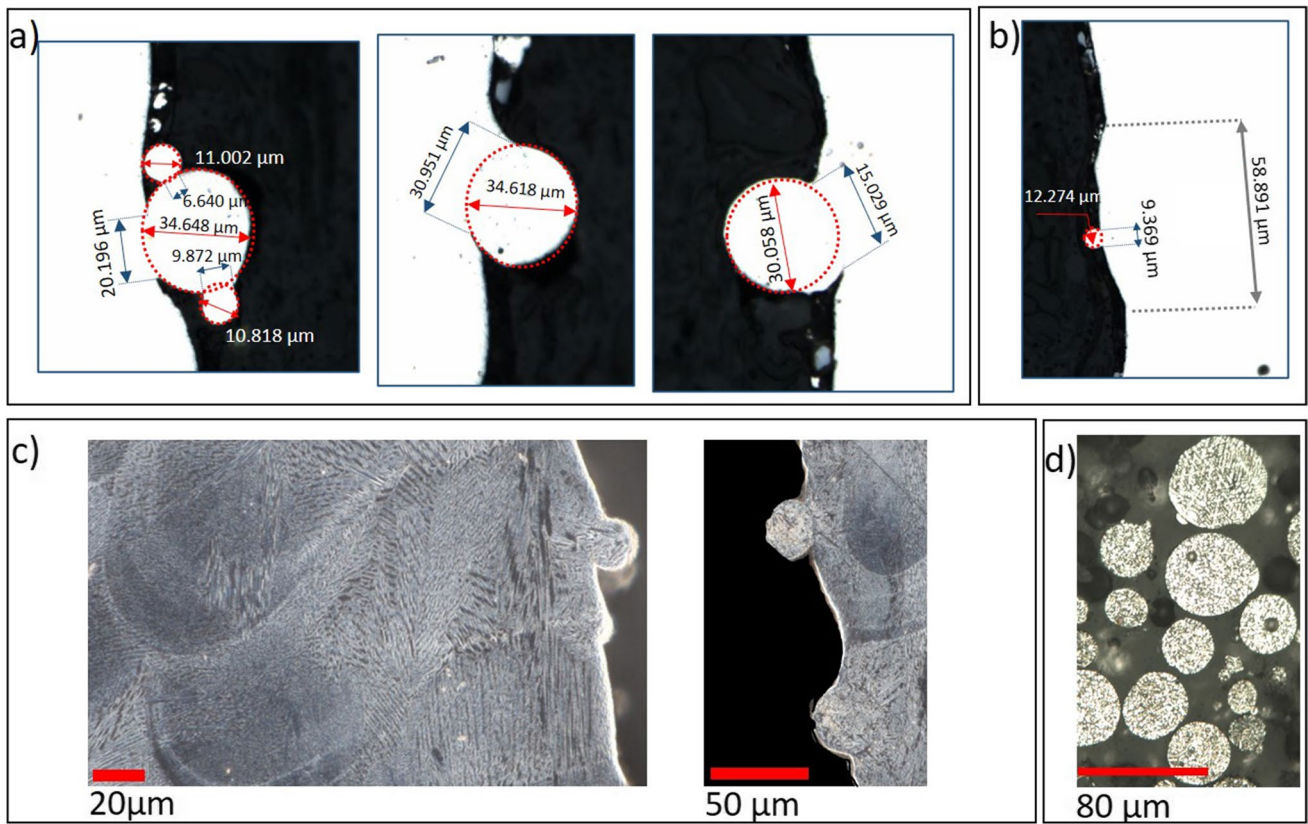


Fig. 8 Metallographic images of adhered particles: **a** adhered particles, **b** adhered particles and surface layers, **c** images of the adhered particles after being etched and **d** analysis of powder particles

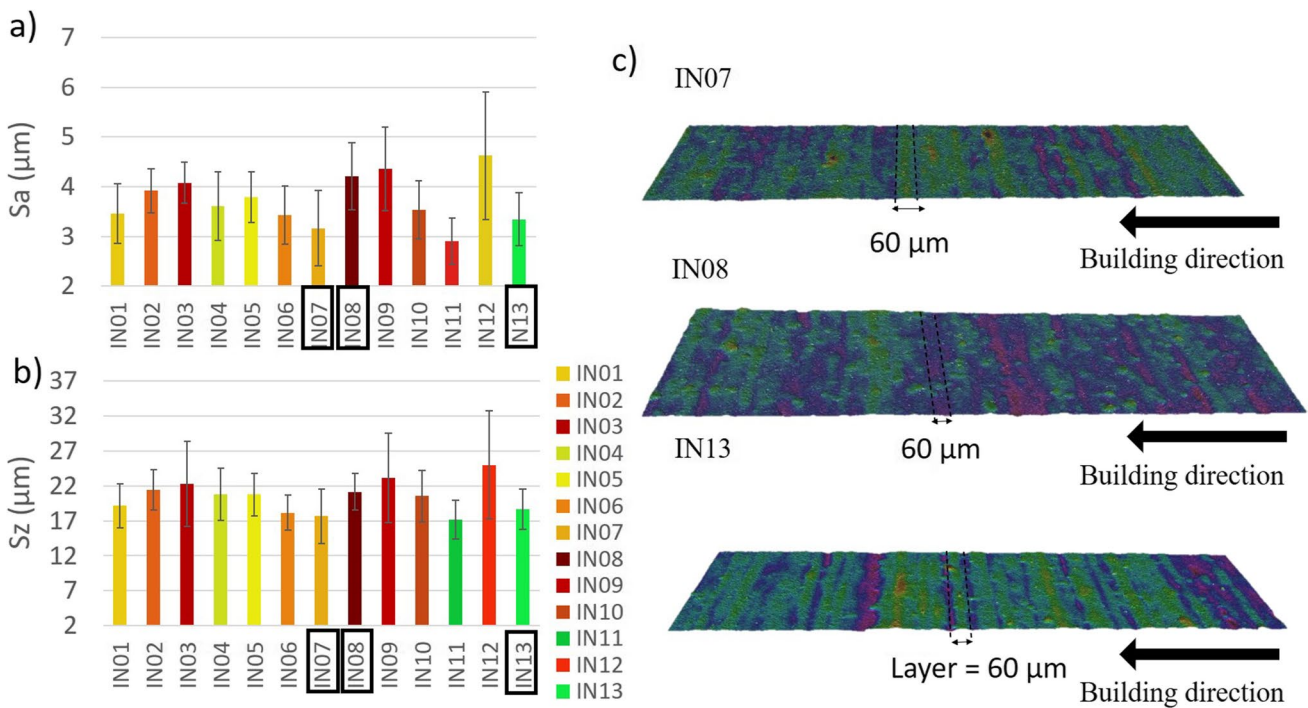


Fig. 9 Roughness of parts after sandblasting: **a** Sa, **b** Sz, and **c** surface images of parts obtained using batches IN07, IN08, and IN13 after sandblasting

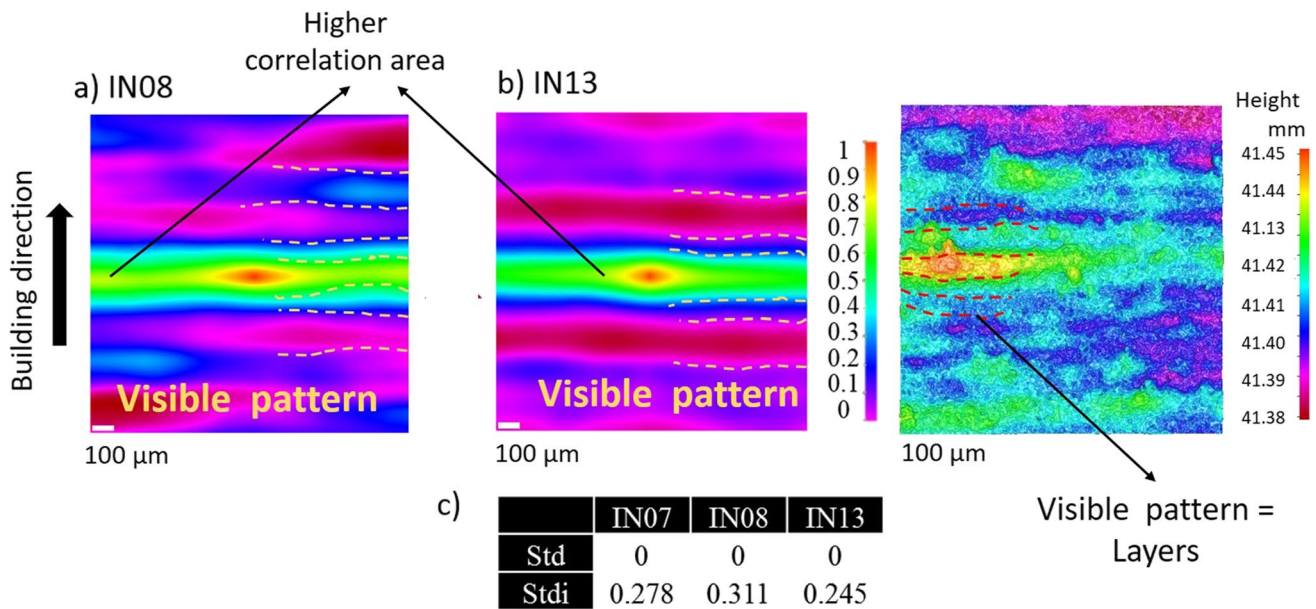


Fig. 10 Analysis of spatial parameters and autocorrelation of the surfaces: **a** autocorrelation diagram of IN08 batch, **b** autocorrelation diagram of IN13 batch and the surface image obtained after sandblasting, and **c** spatial parameters

The Std parameter indicates the predominant direction of surface texture, and, as can be seen, it follows the building direction. In addition, by removing the particles adhered to the surface but keeping the layers, the weight of the directionality increases as the Stdi parameter indicates (Fig. 10(c)). The small differences in the Stdi parameter demonstrate the effect of removing the particles in the pattern composed of layers.

4 Conclusions

This work presents the correlation between the characteristics of the powder used and the surface roughness obtained in the case of manufacturing Inconel® 718 parts using L-PBF technology. The main conclusions drawn are summarised as follows:

- The size of the adhered particles on the surface corresponds to the particle size of the smallest particles of the powder batch. Because smaller particles are more likely to partial melting at the contour of each layer due to heat transfer between the molten material and the powder bed.
- There is a linear relationship between the smallest particles in the powder batch and the surface roughness (S_a). This relationship is only valid for the smallest particles because these particles are the ones that adhere to the surface. In respect to particle sizes above D_{50} , there is no such correlation.

- In powder batches with larger, small particles, the adhered particles are also larger in diameter; therefore, layers cannot be appreciated as easily as on surfaces where only very fine particles were adhered.
- After sandblasting the parts, the particles are removed from the surface, and the roughness of different samples is decreased and homogenized.
- After studying the autocorrelation and spatial parameters of the samples after blasting, it was found that the adhered particles disappear but that the layers are still present on the surface.

Therefore, this study demonstrates the relationship between the roughness and PSD of the powder batch.

Acknowledgements The authors thank to the Spanish Ministry of Science and Innovation for the financial of the grant PRE2020-092632 associated to ALASURF project PID2019-109220RB-I00. Open access funding provided by UPV/EHU.

Author contribution All authors contributed to the study conception and design. Material preparation, data collection, and analysis were performed by Sara Sendino and Silvia Martinez. Marc Gardon and Fernando Lartategui supervised the findings of this work and proposed several analyses. Javier Jesus Gonzalez and Aitzol Lamikiz were involved in planning and supervised the work. The first draft of the manuscript was written by Sara Sendino, and all authors commented on previous versions of the manuscript. All authors read and approved the final manuscript.

Funding Open Access funding provided by UPV/EHU thanks to the CRUE-CSIC agreement with Springer Nature. This research was funded by the Basque Government under the ELKARTEK Program, EDISON project, grant number KK-2022/00070.

Declarations

Competing interests The authors declare no competing interests.

Open Access This article is licensed under a Creative Commons Attribution 4.0 International License, which permits use, sharing, adaptation, distribution and reproduction in any medium or format, as long as you give appropriate credit to the original author(s) and the source, provide a link to the Creative Commons licence, and indicate if changes were made. The images or other third party material in this article are included in the article's Creative Commons licence, unless indicated otherwise in a credit line to the material. If material is not included in the article's Creative Commons licence and your intended use is not permitted by statutory regulation or exceeds the permitted use, you will need to obtain permission directly from the copyright holder. To view a copy of this licence, visit <http://creativecommons.org/licenses/by/4.0/>.

References

- Wang Z, Guan K, Gao M et al (2012) The microstructure and mechanical properties of deposited-IN718 by selective laser melting. *J Alloys Compd* 513:518–523. <https://doi.org/10.1016/j.jallcom.2011.10.107>
- Khorasani AM, Gibson I, Veetil JK, Ghasemi AH (2020) A review of technological improvements in laser-based powder bed fusion of metal printers. *Int J Adv Manuf Technol* 108:191–209. <https://doi.org/10.1007/s00170-020-05361-3>
- Riener K, Albrecht N, Ziegelmeier S et al (2020) Influence of particle size distribution and morphology on the properties of the powder feedstock as well as of AlSi10Mg parts produced by laser powder bed fusion (LPBF). *Addit Manuf* 34:101286. <https://doi.org/10.1016/j.addma.2020.101286>
- Fox JC, Moylan SP, Lane BM (2016) Effect of process parameters on the surface roughness of overhanging structures in laser powder bed fusion additive manufacturing. *Procedia CIRP* 45:131–134. <https://doi.org/10.1016/j.procir.2016.02.347>
- Greitemeier D, Dalle Donne C, Syassen F et al (2016) Effect of surface roughness on fatigue performance of additive manufactured Ti–6Al–4V. *Mater Sci Technol* 32:629–634. <https://doi.org/10.1179/1743284715Y.0000000053>
- Vilardell AM, Krakhmalev P, Fredriksson G et al (2018) Influence of surface topography on fatigue behavior of Ti6Al4V alloy by laser powder bed fusion. *Procedia CIRP* 74:49–52. <https://doi.org/10.1016/j.procir.2018.08.028>
- Jamshidinia M, Kovacevic R (2015) The influence of heat accumulation on the surface roughness in powder-bed additive manufacturing. *Surf Topogr Metrol Prop* 3:14003. <https://doi.org/10.1088/2051-672X/3/1/014003>
- Rott S, Ladewig A, Friedberger K et al (2020) Surface roughness in laser powder bed fusion – Interdependency of surface orientation and laser incidence. *Addit Manuf* 36:101437. <https://doi.org/10.1016/j.addma.2020.101437>
- Senin N, Thompson A, Leach R (2018) Feature-based characterisation of signature topography in laser powder bed fusion of metals. *Meas Sci Technol* 29. <https://doi.org/10.1088/1361-6501/aa9e19>
- Nguyen QB, Luu DN, Nai SML et al (2018) The role of powder layer thickness on the quality of SLM printed parts. *Arch Civ Mech Eng* 18:948–955. <https://doi.org/10.1016/j.acme.2018.01.015>
- Kleszczynskia S, Ladewigb A, Friedbergerb K et al (2015) Position dependency of surface roughness in parts from laser beam. *Proc 26th Int Solid Free Form Fabr Symp* 360–370
- Fiegl T, Franke M, Körner C (2019) Impact of build envelope on the properties of additive manufactured parts from AlSi10Mg. *Opt Laser Technol* 111:51–57. <https://doi.org/10.1016/j.optlastec.2018.08.050>
- Chen Z, Wu X, Tomus D, Davies CHJ (2018) Surface roughness of selective laser melted Ti-6Al-4V alloy components. *Addit Manuf* 21:91–103. <https://doi.org/10.1016/j.addma.2018.02.009>
- Sendino S, Martinez S, Gardon M, Lartategui F et al (2020) The effect of the laser incidence angle in the surface of L-PBF processed parts. *Coatings* 10:1024. <https://doi.org/10.3390/coatings10111024>
- Sendino S, Martinez S, Lamikiz A et al (2021) Analytical study of the melt pool distortion in the laser powder bed fusion process caused by the angle of incidence of the laser and its effect on the surface finish of the part. *IOP Conf Ser Mater Sci Eng* 1193:012010. <https://doi.org/10.1088/1757-899X/1193/1/012010>
- Nasab MH, Gastaldi D, Lecis NF, Vedani M (2018) On morphological surface features of the parts printed by selective laser melting (SLM). *Addit Manuf* 24:373–377. <https://doi.org/10.1016/j.addma.2018.10.011>
- Ladewig A, Schlick G, Fisser M et al (2016) Influence of the shielding gas flow on the removal of process by-products in the selective laser melting process. *Addit Manuf* 10:1–9. <https://doi.org/10.1016/j.addma.2016.01.004>
- Ali U, Mahmoodkhani Y, Imani Shahabad S et al (2018) On the measurement of relative powder-bed compaction density in powder-bed additive manufacturing processes. *Mater Des* 155:495–501. <https://doi.org/10.1016/j.matdes.2018.06.030>
- Ahmed F, Ali U, Sarker D et al (2020) Study of powder recycling and its effect on printed parts during laser powder-bed fusion of 17–4 PH stainless steel. *J Mater Process Technol* 278:116522. <https://doi.org/10.1016/j.jmatprotec.2019.116522>
- Sendino S, Martinez S, Ukar E, Lamikiz A, Gonzalez JJ (2022) Monitoring of the L-PBF process to analyze the effect of powder bed temperature on parts roughness. *Procedia CIRP* 111:355–358. <https://doi.org/10.1016/j.procir.2022.08.038>
- Spierings AB, Herres N, Levy G (2011) Influence of the particle size distribution on surface quality and mechanical properties in AM steel parts. *Rapid Prototyp J* 17:195–202. <https://doi.org/10.1108/13552541111124770>
- Triantaphyllou A, Giusca CL, Macaulay GD et al (2015) Surface texture measurement for additive manufacturing. *Surf Topogr Metrol Prop* 3. <https://doi.org/10.1088/2051-672X/3/2/024002>
- Mumtaz K, Hopkinson N (2009) Top surface and side roughness of Inconel 625 parts processed using selective laser melting. *Rapid Prototyp J* 15:96–103
- Jacobsmühlen J, Kleszczynski S, Ladewig A et al (2016) In-situ surface roughness measurement of laser beam melted parts – a feasibility study of layer image analysis. In: Fraunhofer IWU, Müller B (eds.) *Proc. of the Fraunhofer Direct Digital Manufacturing Conference*. Fraunhofer Verlag, pp 231–240
- Li BQ, Li Z, Bai P et al (2018) Research on surface roughness of AlSi10Mg parts fabricated by laser powder bed fusion. *Metals (Basel)* 8:1–10. <https://doi.org/10.3390/met8070524>
- Leach R (2013) Characterisation of areal surface texture. <https://doi.org/10.1007/978-3-642-36458-7>
- Lou S, Zhu Z, Zeng W et al (2021) Material ratio curve of 3D surface topography of additively manufactured parts: An attempt to characterise open surface pores. *Surf Topogr Metrol Prop* 9. <https://doi.org/10.1088/2051-672X/abedf9>

Publisher's note Springer Nature remains neutral with regard to jurisdictional claims in published maps and institutional affiliations.